Plasmonics
DOI 10.1007/s11468-014-9830-0

Nanoplasmonic Enhancement of Molecular Fluorescence: Theory and Numerical Modeling

Khai Q. Le

Received: 3 September 2014 / Accepted: 2 November 2014

Abstract Significant emission enhancement of fluorescent molecules placed in close proximity to metallic nanoparticles has been observed. Recent advances in nanotechnology have enabled the introduction of plasmon-enhanced molecular fluorescence in various applications. Comprehensive theory of the physics behind this enhancement mechanism has also been developed. However, most of the existing analytical tools are applicable mainly for particular nanoparticles in either spherical or ellipsoidal shapes. Since the plasmonic enhancement of molecular fluorescence is dependent on various parameters such as shape, size, and distribution of nearby nanoparticles, it is crucial to have more powerful analysis tools to be able to handle any arbitrary nanoparticles. For this purpose, the 3D finite element method, which is a commonly used technique for arbitrary structures, is implemented and reported in this paper. The emitting molecule is assumed to be an electric dipole point source. The fluorescence enhancement factor is described in term of a local electric field-enhancement factor and the quantum yield of the system. The model is validated by comparison to the approximate quasistatic model and the exact Mie theory. It provides more accurate results than those of the quasistatic model, which makes it become the powerful numerical approach for investigation of arbitrary nanostructure influence on molecular fluorescence. It is then applied for investigating the emission characteristics of the fluorescent molecule when it is placed in the vicinity of more complicated structures including dimers and chains of coupled nanoparticles. It is found that these coupled nanoparticle configurations provide stronger fluorescence enhancement than the single nanoparticle of the same particle size when the inter-particle gap is small. It is attributed to the higher electric-field enhancement in the inter-particle gap region via strong surface plasmon coupling effects of two neighboring nanoparticles.

Keywords Plasmon-enhanced fluorescence · Mie theory · Quasistatic model · Finite element method

Introduction

Since the pioneering work of Purcell in 1946 that the spontaneous emission rate of a single emitter, e.g., atom, molecule, and quantum dot, could be amplified by resonant coupling to the external environment, tremendous research and development have arisen based on this effect, the so-called Purcell effect or the molecular fluorescence [1]. It means that the lifetime of a molecule excited state depends not only on the molecule itself but also on its surrounding environment. The lifetime is controlled by both the radiative decay rate corresponding to photon emission and the nonradiative decay rate corresponding to energy dissipation into the external environment. It has been observed that the spontaneous emission of the single fluorescent emitter is dramatically enhanced when it is coupled to resonant cavities [2, 3], photonic crystals [4–6], semiconductor quantum wells [7–9], metallic nanoparticles, and surface or multilayer metal structures [10–20].

Among those, plasmonic enhancement of molecular fluorescence near metallic nanoparticles has received much interest due to its widespread utility in measurements and devices in various fields such as chemistry, molecular biology, photonics, medicines, and material sciences [21]. In particular, it has been used to enhance subwavelength imaging of local electromagnetic field and probing of nanostructures [22, 23].

K. Q. Le
Faculty of Science and Technology, Hoa Sen University, Ho Chi Minh, Vietnam

K. Q. Le (✉)
Department of Electrical Engineering, University of Minnesota, Duluth, MN 55812, USA
e-mail: khaidotle@gmail.com

Published online: 18 November 2014

Many other practical applications based on this fluorescence enhancement have been found including surface plasmon enhancement of light emitting diodes (LEDs) [24–26], photonic crystal lasers [27], and up-conversion luminescence for improving solar cell efficiency [28–30].

Influence of metallic nanoparticles on the fluorescent emission of nearby molecules can happen in several ways including (i) an enhancement of the incident light intensity excited on the molecule via near-field enhancement near nanoparticles which changes the probability of spontaneous photon emission, (ii) a modification of the radiative decay rate of the molecule, and (iii) an increase in the coupling efficiency of the fluorescence emission to the far-field via nanoparticle scattering [21]. All these effects can be modified by shape, size, distribution of nanoparticles, and distance of fluorescent molecules to nanoparticles. These structural parameters of nanoparticles determine their optical properties including localized surface plasmon resonance modes excited by an external field. It has been demonstrated in systems of specially sized and arranged nanoparticles that at certain plasmon resonance frequencies, the light intensity in the near-field of the nanoparticle could be enhanced up to 10^2 times for a single nanoparticle (sphere or spheroid) [31], 10^3 times for two coupled nanospheres [32], and 10^6 times for a chain of coupled nanospheres [33] compared to the incident field. Moreover, the enhancement of fluorescence is obtained when the fluorescent molecule is placed in close proximity to the nanoparticle at a distance of a few nanometers [34, 35]. However, there are also existing other cases that the fluorescence is quenched in a certain small molecule-nanoparticle separation [36, 37]. The quenching and enhancement happen in different ranges of distances. It is attributed to the fact that the fluorescence is the product of two processes including the excitation and emission mechanism. In the excitation mechanism, the molecule is excited by the incident field, which is further enhanced by the external environment, e.g., plasmon resonances of the nanoparticle. Whereas, in the emission mechanism, the molecule emits photon radiation, which is influenced by the balance of radiative and nonradiative decay rate [34, 38]. In addition, the scattering efficiency of nanoparticles strongly effects on the fluorescence of nearby molecules. The strong scattering results in the strong coupling of the fluorescence emission to the far-field lead to the enhancement of molecular fluorescence [39]. Therefore, in order to have a comprehensive understanding of the electromagnetic interaction between emitters and metallic nanostructures, it is crucial to study the dependence on plasmon energy and nanoparticle-scattering efficiency of the plasmon-enhanced molecular fluorescence. A deeper understanding of this interaction will provide more opportunities to optimize this fluorescence enhancement for many practical molecule-based measurement and device applications.

There has been extensive theoretical and experimental research on the influence of metallic nanoparticles on the molecular fluorescence. Among those, much attention is paid for a composed system of strongly coupled nanoparticles, e.g., dimers and a molecule [40–44], since these coupled nanoparticles result in strong near-field enhancement in inter-particle gap regions. One of the most widely used analytical methods to deal with dimers is the generalized Mie theory [45, 46]. However, most of these nanoparticles are in spherical shapes and in particular alignment, while other nanoparticle shapes and distribution such as bowtie and aligned nanowires may offer more enhancement of molecular fluorescence, since they are able to ultimately enhance the near-field via anomalous strong surface plasmon coupling [47]. These plasmonic nanoantennas produce amplified local fields, particular when proper pumped resonantly, leading to enhance Raman scattering [48]. Several theoretical and numerical methods including the Green's tensor method [49], the boundary element method (BEM) [50], the finite difference time domain (FDTD) method [51], the finite integration technique (FIT) [52], and the finite element method (FEM) [53] have been employed to model the composed systems of molecules and nanoparticles with the elaborated geometries and arbitrary shapes. Among them, the FDTD and FEM methods are commonly used for the analysis of irregular geometric particles and most of the commercial modeling tools based on. However, the FDTD method may be non-ideal for dealing with the curved geometries such as spheres and ellipsoids since its discretization technique may cause computational errors due to staircase effects. In contrast, the FEM method is more suitable for investigating the curved geometries since its meshing technique employs tetrahedra to smoothly follow curved boundaries, which provides higher spatial resolution and quantitative accuracy [53]. Previous theoretical research on the fluorescent molecule-nanoparticle interaction based on the FEM method was limited to how power and scattered field were radiated to the far-field. There are no prior FEM-based works to predict plasmonic enhancement of molecular fluorescence caused by complex metallic nanostructures. In addition, the light emission source of the fluorescent molecule was assumed to be a line source of an electric dipole with a finite length of 1A or 1 nm while it should be a point source in nature. Indeed, a length of line source may effect on calculated molecular fluorescence [53].

In this work, I investigate several plasmonic nanostructures that are promising to significantly enhance the molecular fluorescence using the FEM method. In contrast to the previous works using a line source for light emission, a point source is used in this work. The model is validated by comparing to the exact electrodynamical theory (Mie theory) [54] and the quasistatic model [55, 56] for a single sphere-molecule case. Here, I study the plasmonic enhancement of the molecular fluorescence caused by a dimer and a chain of coupled

nanoparticles. The results indicate that a huge fluorescence enhancement of >3000 is obtained as the molecule is placed in small inter-particle gap regions while that of a single nanoparticle case is just about 9. It is attributed to the fact that in these areas, the ultimately high electric-field enhancement is achieved due to the extremely strong surface plasmon coupling of the neighboring nanoparticles.

Methods

The overall fluorescence yield, a key parameter determines the fluorescent characteristic of an elementary emitter (molecule, atom, or quantum dot), is based on the product of two factors: the intensity enhancement factor (G) for the excitation light and the quantum yield (Q) of the emitter in the vicinity of metallic nanoparticles. Given the driving field to be in the same direction as the molecular dipole moment, the overall fluorescence yield or the fluorescence enhancement factor (F) is described as follows:

$$F = GQ = \left|\frac{E}{E_0}\right|^2 \left(\frac{\gamma^{\mathrm{R}}}{\gamma^{\mathrm{R}} + \gamma^{\mathrm{NR}}} = \frac{\gamma^{\mathrm{R}}}{\gamma^{\mathrm{tot}}}\right), \tag{1}$$

where E (E_0) is the electric field with (without) metallic nanoparticles; γ^{R}, γ^{NR}, and γ^{tot} are the radiative, nonradiative, and total decay rates of the molecule-nanoparticle system, respectively. The ratio of the radiative to the total decay rates is defined as the quantum yield along with an assumption of the intrinsic quantum yield of the molecule to be unity. In the following sections, the exact Mie theory and the quasistatic model for a single spherical nanoparticle influence on the molecular fluorescence are briefly presented. These analytical models are used to validate the FEM model. Then, the FEM model will be employed to investigate more complicated metallic nanostructures for plasmonic enhancement of the molecular fluorescence. In these models, the external excitation of the electric field is considered to be a plane wave (E= 1 V/m). The molecule is assumed to be a dipolar source. All simulation results are done for the electric field which is linearly polarized along the dipole orientation corresponding to the radial dipole orientation while those for the tangential dipole orientation are neglected. The tangential dipole orientation was ignored since the excitation under this condition does not yield strong nanoparticle coupling, especially for systems consisting of coupled nanoparticles, which are mainly investigated in this work [43, 57].

Electrodynamical Theory

In this section, the exact solution for the light-spherical nanoparticle interaction problem is presented. It is usually employed to compute the overall fluorescence yield $F=GQ$. Since the emitting light from the molecule can be assumed to be an ideal dipole, the problem is resumed to be a dipole-sphere interaction, which can be solved exactly by the Mie theory [58]. For a radial dipole located outside the sphere in vacuum at a position r, the electric-field enhancement factor G for an excited plane wave of frequency ω_{exc} is given by [54]:

$$G(\omega_{\mathrm{exc}}, r) = \left|\frac{E}{E_0}\right|^2 = \frac{1}{(k_{\mathrm{exc}}r)^4}\sum_{n=1}^{\infty} n(n+1)(2n+1)\left|\psi_n(k_{\mathrm{exc}}r) + b_n\zeta_n(k_{\mathrm{exc}}r)\right|^2, \tag{2}$$

where n is an angular mode number, $k_{\mathrm{exc}}=\omega_{\mathrm{exc}}/c$ is the wavenumber, c is the speed of light in vacuum, the function $\Psi_n(k_{\mathrm{exc}}r)=(\pi k_{\mathrm{exc}}r/2)^{1/2}J_{n+1/2}(k_{\mathrm{exc}}r)$ with $J_{n+1/2}(k_{\mathrm{exc}}r)$ being the spherical Bessel function, the function $\zeta_n(k_{\mathrm{exc}}r)=(\pi k_{\mathrm{exc}}r/2)^{1/2}H^{(1)}{}_{n+1/2}(k_{\mathrm{exc}}r)$ with $H^{(1)}{}_{n+1/2}(k_{\mathrm{exc}}r)$ being the spherical Hankel function of the first kind [59], and b_n is the Mie coefficient defined as follows:

$$b_n = -\frac{\sqrt{\varepsilon(\omega_{\mathrm{exc}})}\psi_n\left(k_{\mathrm{exc}}R\sqrt{\varepsilon(\omega_{\mathrm{exc}})}\right)\psi_n'(k_{\mathrm{exc}}R) - \psi_n'\left(k_{\mathrm{exc}}R\sqrt{\varepsilon(\omega_{\mathrm{exc}})}\right)\psi_n(k_{\mathrm{exc}}R)}{\sqrt{\varepsilon(\omega_{\mathrm{exc}})}\psi_n\left(k_{\mathrm{exc}}R\sqrt{\varepsilon(\omega_{\mathrm{exc}})}\right)\zeta_n'(k_{\mathrm{exc}}R) - \psi_n'\left(k_{\mathrm{exc}}R\sqrt{\varepsilon(\omega_{\mathrm{exc}})}\right)\zeta_n(k_{\mathrm{exc}}R)}, \tag{3}$$

where R is the sphere radius and $\varepsilon(\omega_{\mathrm{exc}})$ is the nanoparticle dielectric permittivity.

To determine the quantum yield Q, we need to compute the radiative, nonradiative, as well as the total decay rates of a molecule near a metallic sphere. They are calculated based on the rate of energy carried away from the molecule. The radiative rate is determined by the energy radiated to infinity (or far-field), while the nonradiative rate is calculated by the energy lost in the form of Joule heat into any dissipative medium present. Then, the total rate is given by $\gamma^{\mathrm{tot}}=\gamma^{\mathrm{R}}+\gamma^{\mathrm{NR}}$. With a given decay rate γ_0 in the absence of the sphere, we obtain [52, 54]

$$\frac{\gamma^R(\omega_{\mathrm{emi}}, r)}{\gamma_0} = \frac{3}{2(k_{\mathrm{emi}}r)^4}\sum_{n=1}^{\infty} n(n+1)(2n+1)\left|\psi_n(k_{\mathrm{emi}}r) + b_n\zeta_n(k_{\mathrm{emi}}r)\right|^2, \tag{4}$$

and

$$\frac{\gamma^{\mathrm{tot}}(\omega_{\mathrm{emi}}, r)}{\gamma_0} = 1 + \frac{3}{2(k_{\mathrm{emi}}r)^4}\mathrm{Re}\sum_{n=1}^{\infty} n(n+1)(2n+1)b_n\zeta_n(k_{\mathrm{emi}}r)^2, \tag{5}$$

where $k_{emi}=\omega_{emi}/c$ is the wavenumber, ω_{emi} is the frequency of the emitted light and b_n is the Mie coefficient defined as in Eq. 3 but replacing k_{exc} by k_{emi}. Hence, the quantum yield Q is given by:

$$Q(\omega_{emi}, r) = \frac{\gamma^R(\omega_{emi}, r)}{\gamma^{tot}(\omega_{emi}, r)} = \frac{\frac{\gamma^R(\omega_{emi}, r)}{\gamma_0}}{\frac{\gamma^{tot}(\omega_{emi}, r)}{\gamma_0}}. \quad (6)$$

Quasistatic Model

The quasistatic model was introduced by Gersten and Nitzan, which is accurate for spheres with radius R much smaller than the wavelength of light ($R << \lambda_{exc}, \lambda_{emi}$) [55]. In this model, retardation effects are omitted so that the problem can be solved using the electrostatic approach. The nearby molecule is assumed to be an oscillating point dipole. With these assumptions, the G factor for the molecule placed at a position r near a sphere with radius R *in free space*, made of a material with dielectric permittivity $\varepsilon(\omega_{exc})$ is given by:

$$G(\omega_{exc}, r) = \left| 1 + 2\frac{\varepsilon(\omega_{exc})-1}{\varepsilon(\omega_{exc})+2}\left(\frac{R}{r}\right)^3 \right|^2. \quad (7)$$

The spontaneous radiative decay rate of a dot-like molecule in a close proximity to a small sphere ($R << \lambda_{exc}, \lambda_{emi}$) can be calculated using the following formula:

$$\frac{\gamma^R(\omega_{emi}, r)}{\gamma_0} = \left| 1 + 2\frac{\varepsilon(\omega_{emi})-1}{\varepsilon(\omega_{emi})+2}\left(\frac{R}{r}\right)^3 \right|^2, \quad (8)$$

while the formula to calculate the total decay rate of the molecule is written as

$$\frac{\gamma^{tot}(\omega_{emi}, r)}{\gamma_0} = 1 + \frac{3}{2(k_{emi}R)^3}\sum_{n=1}^{\infty} n(n+1)\left(\frac{R}{r}\right)^{2n+4} \mathrm{Im}\left(\frac{\varepsilon(\omega_{emi})-1}{\varepsilon(\omega_{emi})+\frac{n+1}{n}}\right). \quad (9)$$

It is seen that from Eq. 9, the total decay rate tends to infinity as the molecule approaches to the nanoparticle surface (r->R). Hence, the quantum yield Q will tend to zero. In this case, the fluorescence is quenched and the most excited molecule energy converts into heat by means of Joule losses (heat losses). The fluorescence quenching causes serious difficulties in the efforts to enhance light emission of the florescent molecule by nearby metallic nanostructures. Since the maximum achievable plasmonic enhancement of the molecular fluorescence is obtained at plasmonic resonance modes of the nearby metallic nanostructures, we need to optimize their geometric parameters including their size, shape, distribution, and molecule-nanostructure separation. This optimization along with encountering the fluorescence quenching issue is really a big challenge in this nanoplasmonic-enhanced molecular fluorescence field. Therefore, the development of theoretical methods that allows the investigation of the interaction of light and metallic nanostructures with arbitrary shapes and distributions is very crucial to enhance light scattering and reduce heat losses (or absorption losses). A better understanding of this interaction will provide more opportunities to maximize the fluorescence enhancement and to minimize the fluorescence quenching.

FEM Model

One of the most efficient numerical methods to deal with arbitrary structures is the FEM method. In this model, the fluorescent molecule is assumed to be an electric dipole source, which has an intrinsic quantum yield of unity (i.e., each photon absorbed by the molecule results in a photon emitted). Given the electric field generated by the electric dipole moment p oriented along the z-axis, the radial component of the near-field electric field is described as [53]

$$E_r = \frac{p}{j2\pi\omega_{emi}\varepsilon_0 r^3}, \quad (10)$$

where r is a distance from the point source to the center of the nanoparticle.

Given a normalized electric field $E_r=1$, we yield the dipole moment as follows:

$$|p| = 2\pi\omega_{emi}\varepsilon_0 r^3. \quad (11)$$

The intensity enhancement from the excited plane wave E measured at the dipole source is given by

$$G(\omega_{exc}, r) = \left|\frac{E}{E_0}\right|^2, \quad (12)$$

while the quantum yield is defined as the ratio of the power radiated to the far-field P_{rad} and the total power consisting of the radiated power and Ohmic loss in the nanoparticle P_{abs} (the power absorbed by the nanoparticle)

$$Q(\omega_{exc}, r) = \frac{P_{rad}}{P_{rad}+P_{abs}}. \quad (13)$$

In all FEM simulations, molecule-nanoparticle systems were embedded within a spherical computational domain that

was bounded by a perfectly matched layer (PML) to prevent unexpected reflections. The radiated power was calculated by integrating the flux of the Poynting vector on a closed spherical surface of an inner bound of PML. The absorbed power was computed by integrating the divergence of the Poynting vector in the nanoparticle. The quantum yield definition can also be considered as the one in the surface plasmon-enhanced Raman scattering field in which it is defined as the ratio of the scattering cross-section and the extinction cross-section of the light-nanoparticle system.

Plasmonic Enhancement of Molecular Fluorescence

Single Sphere

To validate the FEM model, I compared it with the exact Mie theory, and the quasistatic model for investigating the molecular fluorescence of an emitter placed in a close proximity of a single Ag sphere. The composed emitter-sphere system is shown as an inset in Fig. 1. The figure depicts the quantum yield of the emitter placed at a distance dr=10 nm to a Ag sphere of radius R=60 nm with respect to the emission wavelength calculated by the provided three models. The particle size is arbitrary chosen for benchmark purposes. The internal quantum efficiency of the emitter is assumed at 100 %. The complex refractive index of Ag was taken in [60]. In order to take all available modes into account, the angular mode number n=60 was used in the exact and quasistatic model [61]. There is a clear discrepancy in the resulted quantum yield using the quasistatic model compared to others because this model is only accurate for small spheres with radius ≤10 nm. The FEM model provides a better agreement to the exact Mie theory. It can be even more accurate if the meshing resolution is finer. From the figure, it is found that at the emission wavelength 330 nm of the molecule, the emitting light is totally absorbed by the sphere and no light is scattered to the far-field. It corresponds to its quantum yield tend to zero. For wavelengths <330 nm, the small quantum yield corresponds to the small scattering of the sphere. In contrast, for wavelengths >330 nm, the quantum yield gradually increases and becomes broader because of the near-field coupling of the localized electric field of the particle and the emitted field of the emitter. Figure 2 shows the calculated quantum yield of the emitter at the emission wavelength 480 nm with respect to its distance to the sphere's surface (R=60 nm). It again demonstrates that the FEM model provides more accurate results than the quasistatic model and thus confirms its validation. To further convince the FEM's validation, a variation of the fluorescence factor F of the molecule effected by the smaller sphere (R=45 nm) with respect to its distance to the sphere's surface is plotted in Fig. 3. In this simulation, the emission wavelength of the molecule was assumed to be at 480 nm under the excitation plane wave at 410 nm. It is obvious that the FEM model remains in better accuracy than the quasistatic model and is in good agreement with the exact theory.

Dimer of Spheres

After the FEM model for nanoplasmonic enhancement of single-molecule fluorescence is validated, it is applied to investigate more complex nanostructures for fluorescence enhancement. The first nanostructure is examined to be a dimer of two Ag spheres since this structure provides a strong electric-field enhancement in the gap of the dimer. It is promising to yield a strong molecular fluorescence enhancement of the fluorescent molecule when it is properly placed in the inter-particle gap. The dimer is depicted in Fig. 4a. Numerous simulations were carried out for various dimer dimensions,

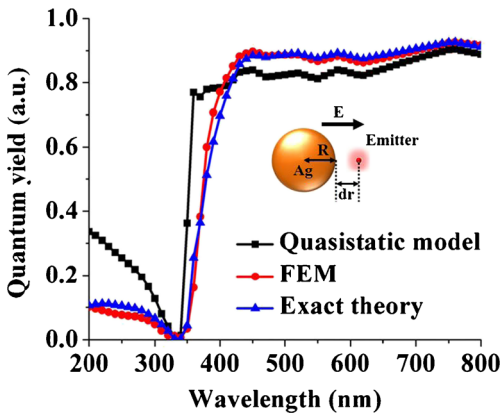

Fig. 1 Dependencies of quantum yield Q on the emission wavelength calculated by the quasistatic model (*black*), the finite element method (*red*), and the exact electrodynamical theory (*blue*), respectively. Inset: an emitter placed near a Ag sphere of radius R=60 nm at a distance to the sphere surface dr=10 nm

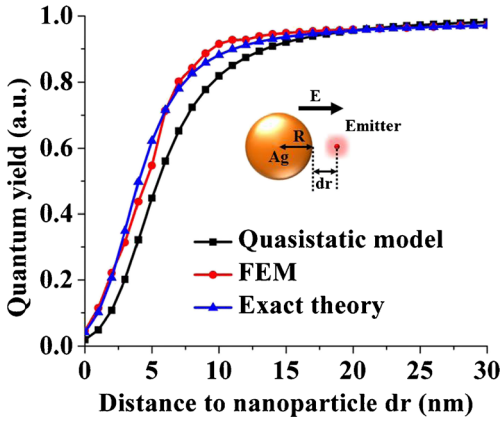

Fig. 2 Variation of quantum yield Q with respect to distance to the sphere surface calculated by the quasistatic model (*black*), the finite element method (*red*), and the exact electrodynamical theory (*blue*), respectively. Inset: a fluorescent molecule emitting at 480 nm placed near a Ag sphere of radius R=60 nm

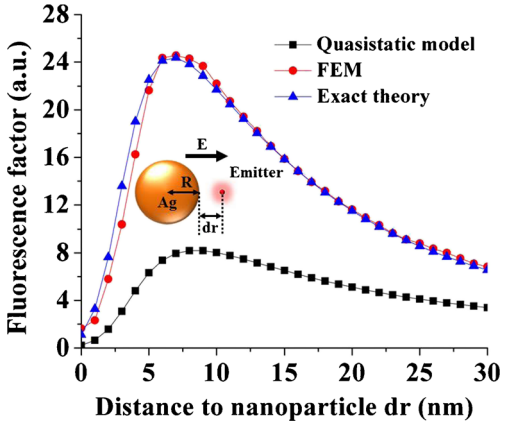

Fig. 3 Variation of fluorescence enhancement factor F with respect to distance to the sphere surface calculated by the quasistatic model (*black*), the finite element method (*red*), and the exact electrodynamical theory (*blue*), respectively. Inset: a fluorescent molecule emitting at 480 nm under the excitation plane wave of λ=410 nm placed near a Ag sphere of radius *R*=45 nm

sphere radius *R* and inter-particle gap dr, to ensure maximum fluorescence factor *F*. Optimization began with a dimer of fixed inter-particle gap dr=3 nm. The highest resulting quantum field was *R*=45 nm, as shown in Fig. 4b. In addition, the closer the nanoparticles, the stronger electric enhancement will be found in the inter-particle gap region, as seen in Fig. 4c. It yields that the fluorescence factor is higher as the molecule is placed inside the smaller inter-particle gap. The fluorescence factor of the dimer is compared to the single sphere of the same radius, as shown in Fig. 5b. For a large distance to the sphere surface dr >17 nm, the dimer acts as an individual sphere; while for a short distance dr ≤17 nm, the increased capacitive coupling of two neighboring spheres results in large electric-field enhancement, as shown in Fig. 5c, which yields higher fluorescence enhancement factor than that of the single sphere. Furthermore, it is seen from Fig. 5d that in the single sphere case, the energy is quenched as the molecule is placed gradually close to the sphere's surface dr <6 nm; whereas in the dimer case, the energy quenching is not visible until dr <1 nm. The dimer provides a significant enhancement of the radiative decay rate and only a marginal enhancement of the nonradiative decay rate compared to the single sphere, which causes no energy quenching until the molecule gets much closer to the sphere's surface.

Chain of Spheres

The second nanostructure is investigated to be a self-similar chain of four Ag spheres. The chain consisting of spheres with progressively decreasing sizes was employed to realize nanolenses in the past. It was demonstrated that in the gap between the smallest spheres, local electric fields were ultimately enhanced by orders of magnitude due to the cascade effects of its geometry and a high Q-factor of the localized surface plasmon resonances [33]. This anomalous feature has inspired several nanofocusing applications. However, the possibility of the enhanced fluorescence using this chain has not been reported. Here, I propose putting the fluorescent molecule in the gap between the smallest nanospheres, as shown in Fig. 5a.

As expected, the molecular fluorescence was significantly enhanced; and thus, the fluorescence enhancement factor is higher than that of the dimer and single sphere. In contrast to the dimer, the chain's *F* factor always surpasses that of the single sphere even if dr >17 nm, as shown in Fig. 5b. It is attributed to the cascade effects of its geometry resulting in a strong electric-field enhancement inside the gap of the smallest spheres. Similar to the dimer, the energy quenching

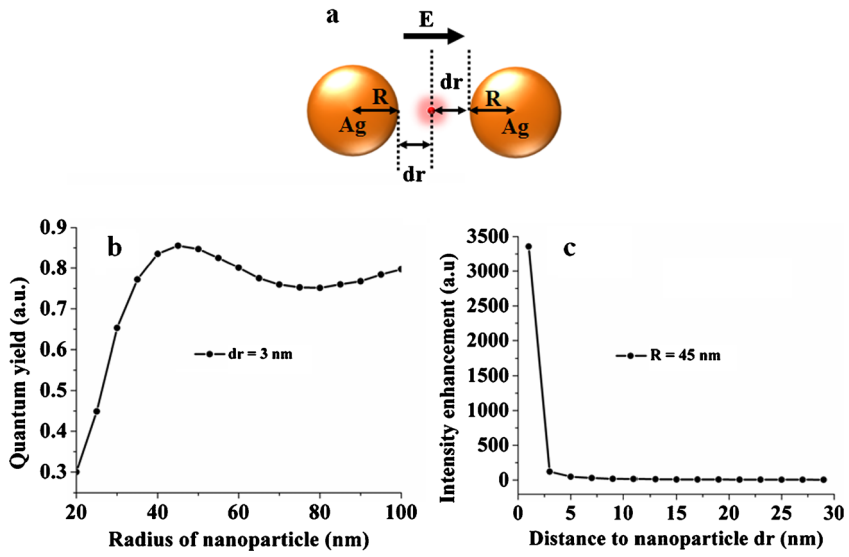

Fig. 4 **a** Sketch of dimer of two Ag nanoparticles where an emitter is placed in the inter-particle gap. **b** Quantum yield Q as a function of radius *R*. **c** Intensity enhancement with respect to distance to the sphere surface dr. An emitter was assumed to emit at 480 nm under the excitation plane wave of λ=410 nm

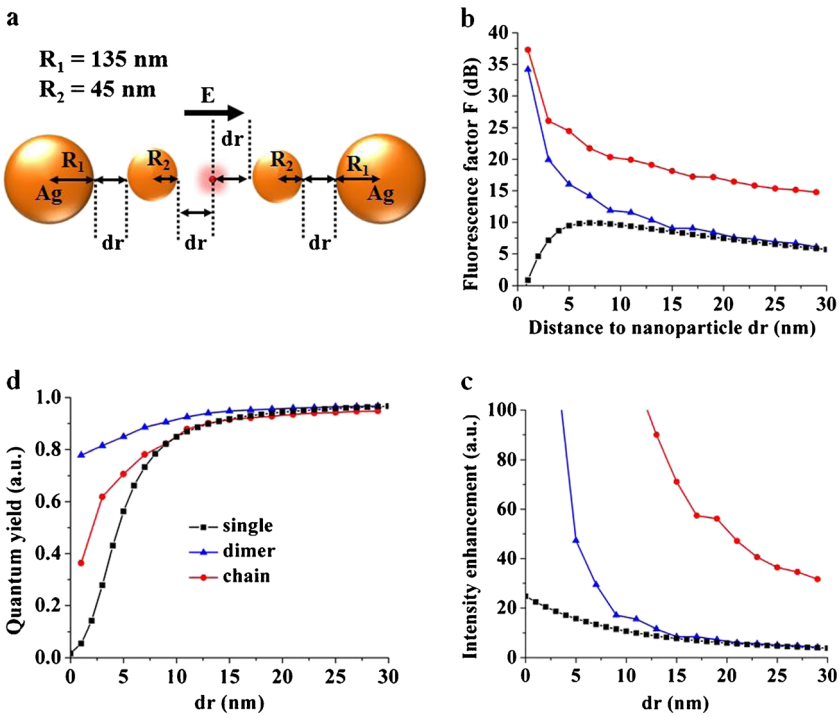

Fig. 5 **a** Geometry of a chain of four Ag spheres where a fluorescent molecule is placed between the gap of two smallest spheres. **b** Fluorescence enhancement factor F, **c** quantum yield Q, and **d** intensity enhancement G of the molecule placed near the single Ag sphere of radius R=45 nm (*black*), the dimer of two Ag sphere of the same radius R (*blue*), and the chain of four Ag spheres of R1= 135 nm and R2=45 nm (*red*) with respect to distance to the sphere surface dr, respectively. The molecule was assumed to emit at 480 nm under the excitation plane wave of λ=410 nm

is not visible until the molecule gets much closer to the sphere's surface (dr <1 nm), as shown in Fig. 5d. Although the quantum yield of the molecule affected by the chain is smaller than that of the dimer, the intensity enhancement caused by the chain is much larger than that of the dimer, which thus results in the higher fluorescence enhancement factor. Since plasmon resonant characteristics of the chain are dependent on size, shape, distribution, and inter-particle gap of nanoparticles, the fluorescence enhancement factor can be obtained at the strongest attitude if the desired emission and excited wavelength are coupled to surface plasmon resonance wavelengths of the chain. In this work, I do not pay much attention on the optimization to achieve the highest enhancement factor; instead, I focus on demonstrating the possibilities to significantly enhance the molecular fluorescence using the investigated chain. Based on the great enhancement of molecular fluorescence by the chain, this system will undoubtedly facilitate the development of new nanoparticle chain-molecule fluorescence toward high-efficiency molecular fluorescence-based measurements and devices [62].

The FEM model highlighted here may allow exploring more complicated plasmonic nanostructures, which is promising to enhance up-conversion of sub-bandgap sunlight. Recently, plasmonic enhancement of light intensity up to 10^3 in up-conversion layer of silicon solar cells has been demonstrated with core-shell ring resonators in near-infrared wavelengths [63]. Plasmonic resonances provide a stronger light concentration essential for a higher efficiency nonlinear optical up-conversion. Along with the model, it allows predicting the up-conversion contributed to the overall photo-current generation efficiency. Much more plasmonic structures, which provide stronger intensity enhancement, will be explored in order to achieve larger conversion efficiencies than what are currently available in energy-harvesting devices, in particular when optimized designs are considered.

Conclusions

In this paper, I have presented a numerical model of enhanced molecular fluorescence near the metallic nanostructures. The model is based on the finite element method, which allows dealing with arbitrary particle geometries. The accuracy of the model was validated by comparing to the exact electrodynamical theory and the existing quasistatic model. The model provided an excellent agreement to the exact solution for the single-molecule fluorescence problem. The model was then employed to investigate complex nanostructures including the dimer and the chain of coupled nanoparticles, which yielded higher fluorescence enhancement of the fluorescent molecule when it was properly placed in the small gap between nanoparticles than that of the single sphere. Among those, the chain of coupled nanoparticles provided possibilities to achieve much higher fluorescence enhancement than others, which were firstly reported in this work. Apparently, the model is very useful to investigate more complicated structures to explore possibilities of enhanced molecular fluorescence.

References

1. Purcell EM (1946) Phys Rev 69:681
2. Goy P, Raimond JM, Gross M, Haroche S (1983) Phys Rev Lett 50: 1903–1906
3. Hulet RG, Hilfer ES, Kleppner D (1985) Phys Rev Lett 55:2137–2140
4. John S (1987) Phys Rev Lett 58:2486–2489
5. Yablonovitch E (1987) Phys Rev Lett 58:2059–2062
6. Boroditsky M, Vrijen R, Krauss TF, Coccioli R, Bhat R, Yablonovitch EJ (1999) Lightwave Technol 17:2096–2112
7. Gerard JM, Sermage B, Gayral B, Legrand B, Costard E, Thierry-Mieg V (1988) Phys Rev Lett 81:1110–1113
8. Gerard JM, Gayral BJ (1999) Lightwave Technol 17:2089–2095
9. Kiraz A, Michler P, Becher C, Gayral B, Imamoglu A, Zhang LD, Hu E, Schoenfeld WV, Petroff PM (2001) App Phys Lett 78:3932–3934
10. Drexhage KHJ (1970) Lumin 1:693–701
11. Kuhn H (1970) J Chem Phys 53:101
12. Agarwal GS (1975) Phys Rev B 12:1475
13. Grossel P, Vigoureux JM, Payen E (1977) Opt Commun 20:192
14. Wylie JM, Sipe JE (1984) Phys Rev A 30:1185
15. Grossel P, Van-Labeke D, Vigoureux JM (1983) Chem Phys Lett 99:193
16. Chew H (1988) Phys Rev A 38:3410
17. Gontijo I, Boroditsky M, Yablonovitch E, Keller S, Mishra UK, DenBaars SP (1999) Phys Rev B 60:11564–11567
18. Chance RR, Prock A, Silbey RJ (1974) Chem Phys 60:2744–2748
19. Dulkeith E, Morteani AC, Niedereichholz T, Klar TA, Felfmann J, Levi SA, van Veggel F, Reinhoudt DN, Moller M, Gittins DI (2002) Phys Rev Lett 89:203002
20. Biteen JS, Lewis NS, Atwater HA, Mertens H, Polman A (2006) Appl Phys Lett 88:131109
21. Tam F, Goodrich GP, Johnson BR, Halas NJ (2007) Nano Lett 7:496–501
22. Betzig E, Chichester R (1993) J Science 262:1422
23. Michaelis J, Hettich C, Mlynek J, Sandoghdar V (2000) Nature 405: 325
24. Okamoto K, Niki I, Shvartser A, Narukawa Y, Mukai T, Scherer A (2004) Nat Matters 3:601–605
25. Catchpole KR, Pillai SJ (2006) Lumin 121:315–318
26. Le KQ, Bienstman P (2011) Plasmonic 6:53–57
27. Painter O, Lee RK, Scherer A, Yariv A, O'Brien JD, Dapkus PD, Kim I (1999) Science 284:1819–1821
28. Fischer S, Steinkemper H, Loper P, Hermle M, Goldschmidt JC (2011) J Appl Phys 111:013109
29. Goldschmidt JC, Fisher S, Steinkemper H, Hallermann F, Plessen Von G, Kramer KW, Biner D, Hermle M (2012) IEEE J Photovolt 2: 134–140
30. Atre AC, Etxarri AG, Alaeian H, Dionne JA (2012) J Opt 14:024008
31. Dynich RA, Ponyavina ANJ (2008) Appl Spectrosc 75:831–837
32. Kottmann JP, Martin OJF (2001) Opt Lett 26:1096–1098
33. Li K, Stockman MI, Bergman D (2003) J Phys Rev Lett 91: 227402
34. Anger P, Bharadwaj P, Novotny L (2006) Phys Rev Lett 96:113002
35. Shimizu KT, Woo WK, Fisher BR, Eisler HJ, Bawendi MG (2002) Phys Rev Lett 89:117401
36. Dulkeith E, Ringler M, Klar TA, Felfmann J, Javier AM, Parak WJ (2005) Nano Lett 5:858–589
37. Trabesinger W, Kramer A, Kreiter M, Hecht B, Wild UP (2002) Appl Phys Lett 81:2118
38. Krug JT, Sanchez EJ, Xei XS (2005) Appl Phys Lett 86:233102
39. Lakowicz JR (2005) Anal Biochem 337:171–194
40. Liaw JW, Chen JH, Chen CS, Kuo MK (2009) Opt Express 17:13532
41. Zoriniants G, Barnes WL, New J (2008) Phys 10:105002
42. Ringler M, Schwemer A, Wunderlich M, Nichtl A, Kurzinger K, Klar TA, Felfmann J (2008) Phys Rev Lett 100:203002
43. Blanco LA, De Garcia Abojo FJ (2004) Phys Rev B 69:205414
44. Chowdhury MH, Pond J, Gray SK, Lakowicz JR (2008) J Phys Chem C 112:11236
45. Xu YL (1995) Appl Opt 34:4573–4588
46. Xu YL (1998) Phys Lett A 249:30–36
47. Kinkhabwala A, Yu Z, Fan S, Avlasevich Y, Mullen K, Moerner WE (2009) W E Nature Photon 3:654–657
48. Willets KA, Van Duyne RP (2007) Annu Rev Phys Chem 58:267–297
49. Martin OJF, Girard C, Dereux A (1995) Phys Rev Lett 74:526–529
50. De Garcia Abojo FJ, Howie A (1998) Phys Rev Lett 80:5180–5183
51. Miao X, Brener I, Luk TSJ (2010) Opt Soc Am B 27:1561–1570
52. Polemi A, Chuford KL (2012) J Chem Phys 136:184703
53. Khoury CG, Norton SJ, Vo-Dinh T (2010) Nanotechnology 21: 315203
54. Kim YS, Leung PT, George TF (1988) Surf Sci 195:1–14
55. Gersten J, Nitzan A (1981) J Chem Phys 75:1139
56. Guzatov DV, Vaschenko SV, Stankevich VV, Lunevich AY, Glukhov YF, Gaponenko SVJ (2012) Phys Chem C 116:10723–10733
57. Chowdhury MH, Pond J, Gray SK, Lakowicz JR (2008) J Phys Chem C 112:11236
58. Mie G (1908) Ann Phys (Leipzig) 25:377–445
59. Abramowitz M, Stegun IA (1965) Handbook of Mathematical Functions. Dover, New York
60. Johnson B, Christy RW (1972) Phys Rev B 6:4370–4379
61. Mertens H, Koenderink AF, Polman A (2007) Phys Rev B 76:115123
62. Valeur B, Berberan MN (2012) Molecular fluorescence: principles and applications. Wiley-VCH, Germany
63. Le KQ, John S (2014) Opt Express 22:A1–A12